Received: Added at production | Revised: Added at production | Accepted: Added at production

DOI: xxx/xxxx

Hidden Tumor Visualization in Augmented Monocular Liver Laparoscopy

Kirana Hanifati[1] | Mohammad Alkhatib[1] | Erol Ozgur[1] | Emmanuel Buc[2] | Bertrand Le Roy[3] | Hestiasari Rante[4] | Youcef Mezouar[1] | Adrien Bartoli[2]

[1]Clermont Auvergne INP, Institut Pascal, Clermont-Ferrand, France

[2]University Hospital, Clermont-Ferrand, France

[3]University Hospital, Saint-Etienne, France

[4]Politeknik Elektronika Negeri Surabaya, Surabaya, Indonesia

Correspondence
Corresponding author Kirana Hanifati,
Email: kirana.hanifati@sigma-clermont.fr

Abstract

We address the hidden tumor visualization problem in augmented monocular liver laparoscopy. Conveying a hidden tumor's depth correctly to the surgeon in augmented monocular laparoscopy is extremely difficult and still forms an unsolved problem. The depth conveyance can be splitted into two subsequent problems. First, designing a visualization that convinces the user to see the tumor inside the organ. Second, enhancing this visualization so that it also provides metric depth perception. The most promising visualization methods rely on a preoperative CT organ model with the tumor to be registered to an intraoperative laparoscopic image. Such a registration allows the organ's intraoperative shape mesh to be overlaid on top of the augmented tumor. The overlaid organ mesh guarantees a partial occlusion on the augmented tumor. This provides a powerful depth cue for the surgeon's perception. However, this type of registration, especially in liver laparoscopy, is usually not real-time and sometimes not possible. This is because of the liver deformation and lack of matchable features between the multimodal images. Subsequently, the tumor augmentation cannot be carried out continuously to guide the surgeon. We propose a novel visualization method to address these limitations. The proposed method replaces the deformable preoperative to intraoperative liver registration with a rigid tumor registration via laparoscopic ultrasound (LUS) imaging. The proposed method handles surgical tool occlusions, runs faster, and outperforms the state of the art in terms of depth perception, as shown in the user study.

KEYWORDS
Augmented Reality, Laparoscopic Surgery, Tumor Visualization

1 | INTRODUCTION

Mini-invasive surgery (MIS) offers significant advantages over open surgery, including reduced complications, shorter hospital stays, and lower costs. However, MIS brings two challenges. First, it prevents the surgeon from palpating organs directly, making it harder to locate tumors inside the organs. Second, while laparoscopic ultrasound (LUS) is a valuable intraoperative tool for real-time visualization of in-organ tumors during MIS, it requires significant expertize to operate effectively. As a result, accurately localizing tumors inside the organ remains a challenging task, even when using LUS.

Augmented reality (AR) guidance can make using LUS easier and help surgeons by giving clear and intuitive visual feedback [1]. AR-guided surgery involves two critical steps. First, *registration*, where preoperative CT scans are aligned with intraoperative laparoscopic images. Second, *visualization*, where the registered tumor is overlaid on the laparoscopic images to show its location. Most of the literature on AR-guided surgery focuses on the registration step and ignores the second yet important visualization step. We address the visualization step in laparoscopic liver surgery. This corresponds to the well-known difficult occluded-object visualization problem in AR (i.e., the occluded object is perceived to float over its occluding surface rather than behind it). This problem does not exist at all in the context of 3D cameras, but is nonetheless highly relevant in monocular liver laparoscopy which uses a standard 2D camera. Specifically, in AR-guided liver surgery, hidden tumor visualization can be split

 © Copyright Holder Name

FIGURE 1 The left image shows a raw laparoscopic liver image. The middle image shows Transparent Overlay visualization of the registered hidden structures such as the tumors (yellow) and veins (blue). The right image shows the overlaid registered liver mesh on top of the augmented hidden structures. Images are taken from paper[2].

into two subsequent problems. First, designing a visualization that convinces the user to see the tumor inside the liver. Second, enhancing this visualization so that it also provides metric depth perception.

Most promising visualization methods rely on a preoperative CT liver model with the tumor to be registered to an intraoperative laparoscopic image. Such a registration allows the liver's intraoperative shape mesh to be overlaid on top of the augmented tumor. The overlaid liver mesh guarantees a partial occlusion of the augmented tumor. This provides a powerful depth cue for the surgeon's perception. An example of this type of visualization can be seen in figure 1 retrieved from paper[2]. The visualization in the right-most image in figure 1 convinces the surgeon to see the tumor inside the liver and not floating over the liver. This is because of three powerful perceptual reasonings. First, the registered liver mesh overlaps the liver surface. Second, the registered liver mesh partially occludes the augmented volumetric tumor. The augmented volumetric tumor is thus perceived behind the registered liver mesh. Third, since the registered liver mesh tightly envelopes the liver surface, the augmented volumetric tumor cannot be between the mesh and the liver surface. Consequently, the augmented volumetric tumor is perceived behind the liver surface.

However, preoperative to intraoperative laparoscopic liver registration is usually neither real-time nor possible for every laparoscopic image. This is because of two reasons. First, the registration has to handle the liver's intraoperative deformation. This is computationally very demanding. Second, preoperative to intraoperative laparoscopic liver registration requires that the liver is visible as much as possible in the laparoscopic image so that the registration succeeds, see figure 1. However, the liver is usually very partially visible in the laparoscopic images. This substantially reduces matchable features between the preoperative liver model and the intraoperative laparoscopic image. Subsequently, the tumor's registration and thus its augmentation cannot be carried out continuously to guide the surgeon.

We propose a novel visualization method to address these limitations with three variant visualizations: *(i)* MoT which stands for "Mesh-over-Tumor", *(ii)* RoT which stands for "ROI-mesh-over-Tumor", and *(iii)* RoT-D which stands for "ROI-mesh-over-Tumor-with-Depth-indicator". The proposed visualization method has two important contributions:

1. It eliminates the deformable preoperative to intraoperative liver registration. Instead, It suggests a rigid tumor registration between three multimodalities: preoperative CT tumor model, intraoperative laparoscopic image, and intraoperative LUS image. This makes it significantly faster and possible even with a very partially visible liver in the laparoscopic image.
2. It handles surgical tool occlusions. This often occurs during the suggested rigid tumor registration process through the use of an LUS probe.

The rest of the paper is organized as follows. Section 2 reviews the related work. Section 3 explains the proposed visualization method. Sections 4 and 5 present the user studies and results. Section 6 concludes the paper and outlines future work.

2 | RELATED WORK

We review related work in surgical AR visualization. Each has its distinct strengths and limitations.

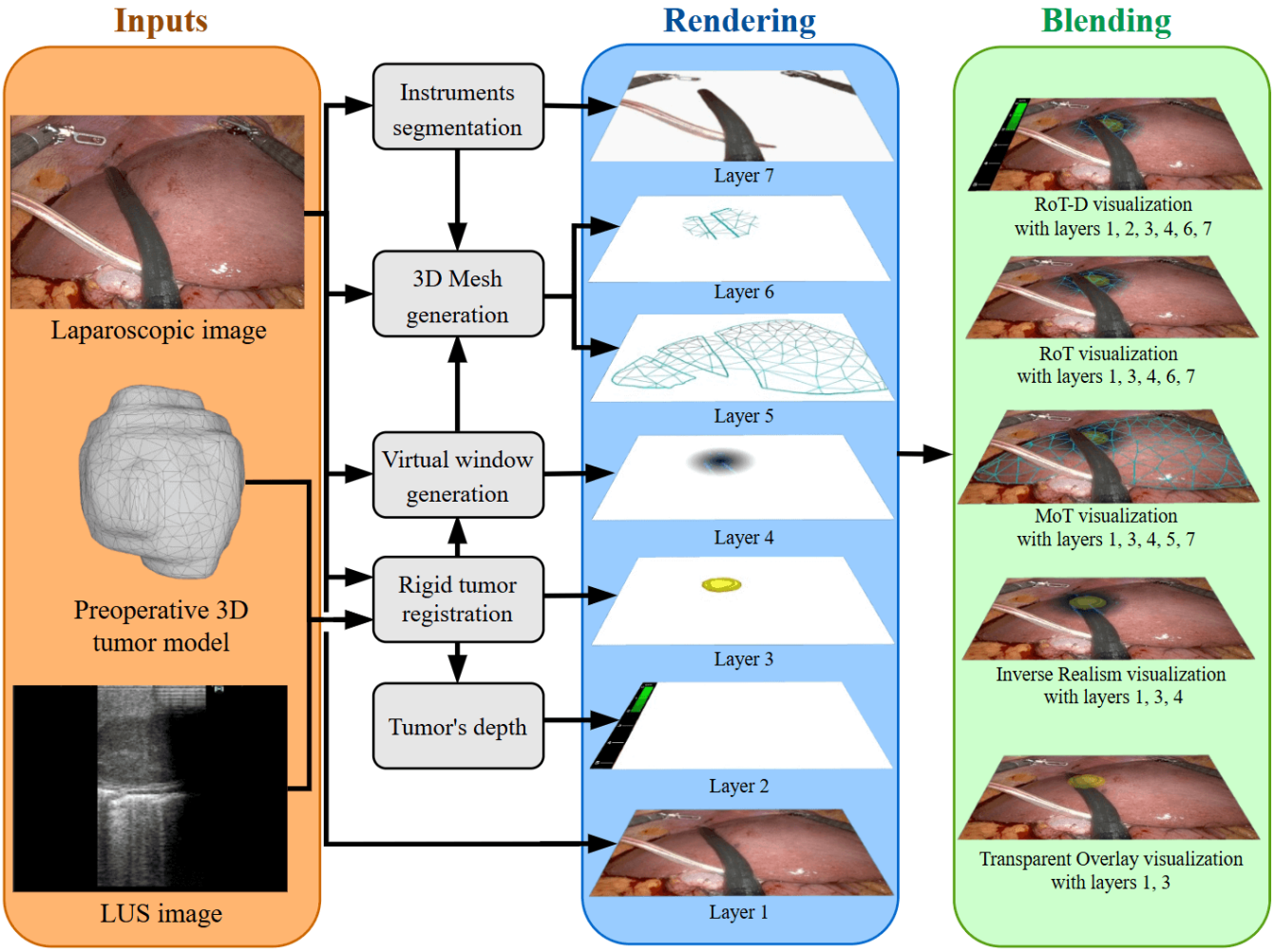

FIGURE 2 The proposed visualization method's pipeline.

Transparent Overlay visualization. In previous work[3,4,5,6,7,8,9,10,11], tumor models are semi-transparently overlaid onto the liver surface, offering positional cues. However, this visualization misrepresents spatial depth relationships. This is because the augmented tumor appears to protrude outside the organ surface and is thus perceived as floating above the organ rather than underneath.

Inverse Realism visualization. This method addresses hidden structures visualization in MIS[12]. It renders the organ's surface textures onto a structure's 3D model using edge features. This creates an 'inverse realism' effect where a hidden structure remains visible with the occluding organ's surface texture. However, when the organ's occluding surface lacks texture, the effect breaks down, and the visualized hidden structure appears floating above the organ.

Visualization via preoperative to intraoperative organ registration. A rigid registration method for uterus tumor localization is proposed in[13], which produces tumor visualizations with correct spatial depth relationships. However, its rigid organ registration would not yield correct tumor localization for the liver. This is because the liver is highly deformable compared to the uterus. A deformable registration method specifically for the liver is presented in[2]. It produces tumor visualizations with correct spatial depth relationships. However, the deformable liver registration is not real-time and cannot be sustained for all laparoscopic images as discussed in the introduction.

3 | METHODOLOGY

The proposed visualization method's pipeline is presented in figure 2. Its inputs are the current intraoperative laparoscopic and LUS images, and the preoperative 3D tumor model.

These inputs undergo several processing steps: *(i)* rigid tumor registration, *(ii)* tumor's depth retrieval, *(iii)* virtual window generation, *(iv)* 3D mesh generation, and *(v)* instrument segmentation. The processed inputs through these steps are then rendered and blended to produce the state-of-the-art visualizations (*i.e.*, Transparent Overlay and Inverse Realism) and the three novel visualizations (*i.e.*, MoT, RoT and RoT-D). We next explain each step below.

Rigid tumor registration. This step registers a rigid preoperative 3D tumor model to a 2D laparoscopic image using an intraoperative LUS image. The 3D tumor model is created from the segmented preoperative CT. This step involves solving two substeps. First, registration of the rigid preoperative 3D tumor model to the LUS image, *e.g.*, similar to [3]. It employs content-based image retrieval (CBIR) to estimate the LUS image's pose on the preoperative CT model [3]. Second, LUS imaging plane's pose computation in the laparoscope's coordinate frame, *e.g.*, similar to [14]. It uses the LUS probe's silhouette contour from the laparoscopic image and employs sequential RANSAC runs on this contour for robust pose estimation [14]. Both [3] and [14] are markerless and trackerless methods. Subsequently, this registration step is feasible in the operating room.

Tumor's depth retrieval. This step retrieves the depth from the registered tumor. The depth is the distance between the LUS sensor and the tumor. We consider that the tumor registration is correct, thus the retrieved tumor depth is correct. However, the tumor's depth accuracy depends on the accuracy of two subsequent methods. *(i)* First, a method used for the segmentation of the tumor in an intraoperative LUS image (*e.g.*, [15] achieves 87% Dice score). *(ii)* Second, a method used for the registration of the 3D tumor model to the segmented intraoperative LUS image (*e.g.*, [3] achieves TRE of 3 *mm*).

Virtual window generation. This step generates a virtual window centered on the rendered tumor's center of mass pixel position. Its size is about 1.5 times of the tumor's rendered size. It also includes the edge features computed from the liver's surface in the laparoscopic image.

3D mesh generation. This step generates two 3D meshes. The first mesh is for the liver's visible surface. The second mesh is for a region of interest (ROI) on the liver's visible surface. Specifically, the ROI corresponds to the virtual window area.

Mesh generation on the liver's visible surface. First, the liver is segmented in the laparoscopic image using MedSAM [16,17,18], a foundation model fine-tuned for laparoscopic imagery. Second, the depth map of the segmented liver is computed using the Depth Anything Model (DAM) [19,20]. The depth map is then used to generate the liver's visible surface 3D mesh. Although this 3D mesh is not very accurate, its rendering perfectly aligns with the segmented liver in the laparoscopic image. See figure 3.

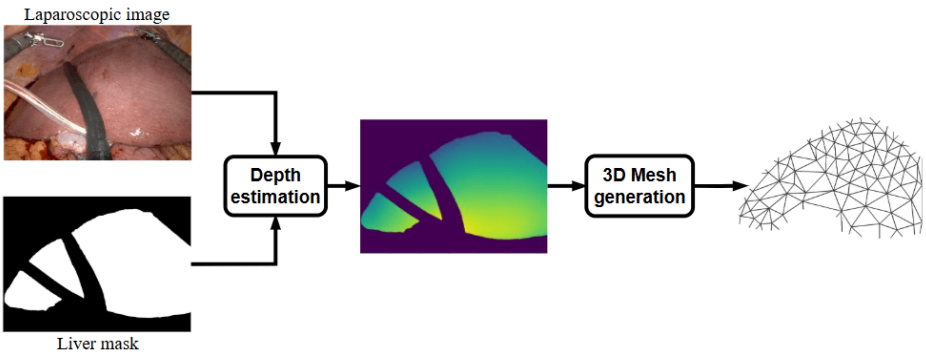

FIGURE 3 3D mesh generation on the liver's visible surface.

ROI mesh generation on the liver's visible surface. Two binary masks, the liver's segmentation mask and the virtual window mask, form the ROI mask using the logical AND operation. Second, the ROI mask, along with the corresponding RGB laparoscopic image, is passed to DAM to compute the ROI depth map. Finally, this is used to generate the ROI 3D mesh. See figure 4.

Instruments segmentation. We know that the visible parts of the surgical instruments occlude everything behind them. Therefore, the instruments' pixels must not be altered [21,22,23]. We find these pixels using SurgicalDeSAM [24]. SurgicalDeSAM is

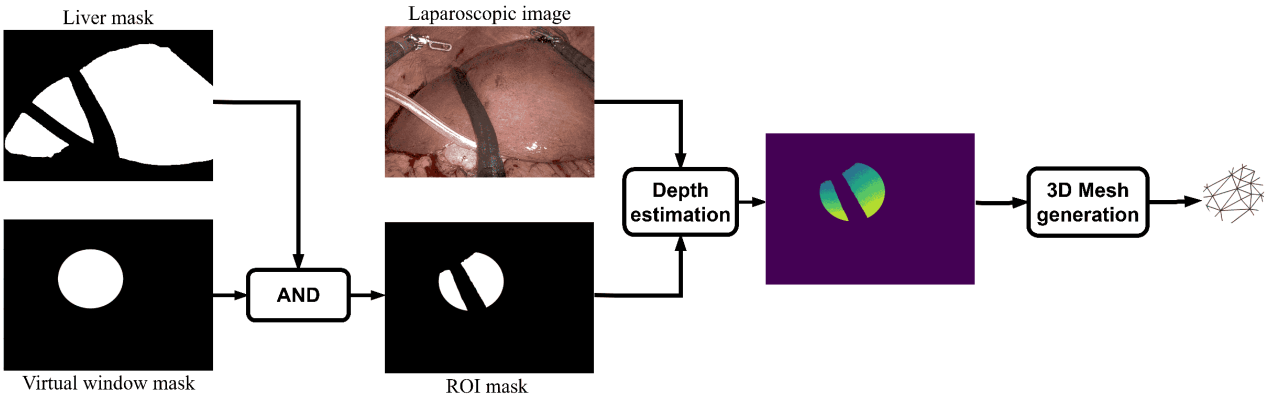

FIGURE 4 ROI 3D mesh generation on the liver's visible surface inside the virtual window.

a foundation model adapted from Segment Anything Model (SAM) and trained on surgical scenes to segment instruments in laparoscopic images. SurgicalDeSAM achieves 90% Dice score for laparoscopic instrument segmentation at 30 fps on EndoVis 2017 and 2018 datasets. Consequently, this step does not form a bottleneck in the pipeline for real-time feasibility.

Rendering. This step renders seven layers: *(i)* input image, *(ii)* tumor's depth bar, *(iii)* tumor, *(iv)* virtual window, *(v)* liver's visible surface mesh, *(vi)* ROI mesh, and *(vii)* instruments. The input image layer is rendered as the original input image. The tumor's depth bar layer is rendered using tumor's depth information. The tumor layer is rendered from the registered tumor. The virtual window layer is rendered from the generated virtual window. The liver's visible surface mesh layer and the ROI mesh layer are rendered from the generated 3D meshes. The instruments layer is rendered from the segmented instruments image.

Blending. This step blends the rendered layers to form five visualizations: *(i)* Transparent Overlay visualization, *(ii)* Inverse Realism visualization, *(iii)* MoT visualization, *(iv)* RoT visualization, and *(v)* RoT-D visualization. Transparent Overlay visualization is blended from the input image and the tumor layers using depth-aware transparency. Inverse Realism visualization is blended from the input image, the tumor and the virtual window layers, as in [12], which has been shown to improve the hidden structures perception. The virtual window, in this visualization, gradually transitions from semi-transparent at the center to fully transparent at the boundary. MoT visualization is blended using the input image, the tumor, the virtual window, the liver's visible surface mesh, and the instruments layers. The liver's visible surface mesh is blended using depth-aware brightness, enhancing the liver's shape perception. RoT visualization is blended using the input image, the tumor, the virtual window, the liver's ROI mesh, and the instruments layers. Again, the ROI mesh is blended using depth-aware brightness. RoT-D visualization is blended using RoT visualization and the tumor's depth bar layer.

Discussion. The proposed visualization method replaces the difficult deformable registration between the preoperative 3D liver model and the intraoperative 2D laparoscopic image, which provides the liver's full shape mesh and the tumor's location, with the 3D mesh generation and the rigid tumor registration steps.

Advantages. There are two advantages. The first advantage is that the proposed method can make AR guidance possible even with a very partially visible liver in the laparoscopic image. This is because rigid tumor registration requires only the LUS probe to be visible in the laparoscopic image. The second advantage is that the proposed method can run significantly faster. This is mainly because it uses a rigid tumor registration and not a deformable liver registration. Each step of the proposed method can be achieved in real time using recent deep learning methods. Specifically, [25] and [26] perform 3D to 2D deformable liver registration at 16 fps and 66 fps, respectively. [15] and [27] segment hepatic intraoperative ultrasound images at 15 fps and 30 fps, respectively. This shows that rigid tumor registration step's real-time feasibility is possible.

Limitations. We list the important limitations of the proposed method. The rigid tumor registration requires detection and segmentation of a tumor in an LUS image. This can be hindered for two reasons. First, LUS images are usually very noisy. Second, the tumor might be isoechoic. In such a case, a potential fallback strategy would use a deformable registration method (*e.g.*, [28],[29]) that aligns a preoperative 3D liver model to the intraoperative laparoscopic image, which does not depend on the LUS image. Afterward the 3D mesh generation requires an accurate liver segmentation. This can be hindered if the laparoscopic image is underexposed.

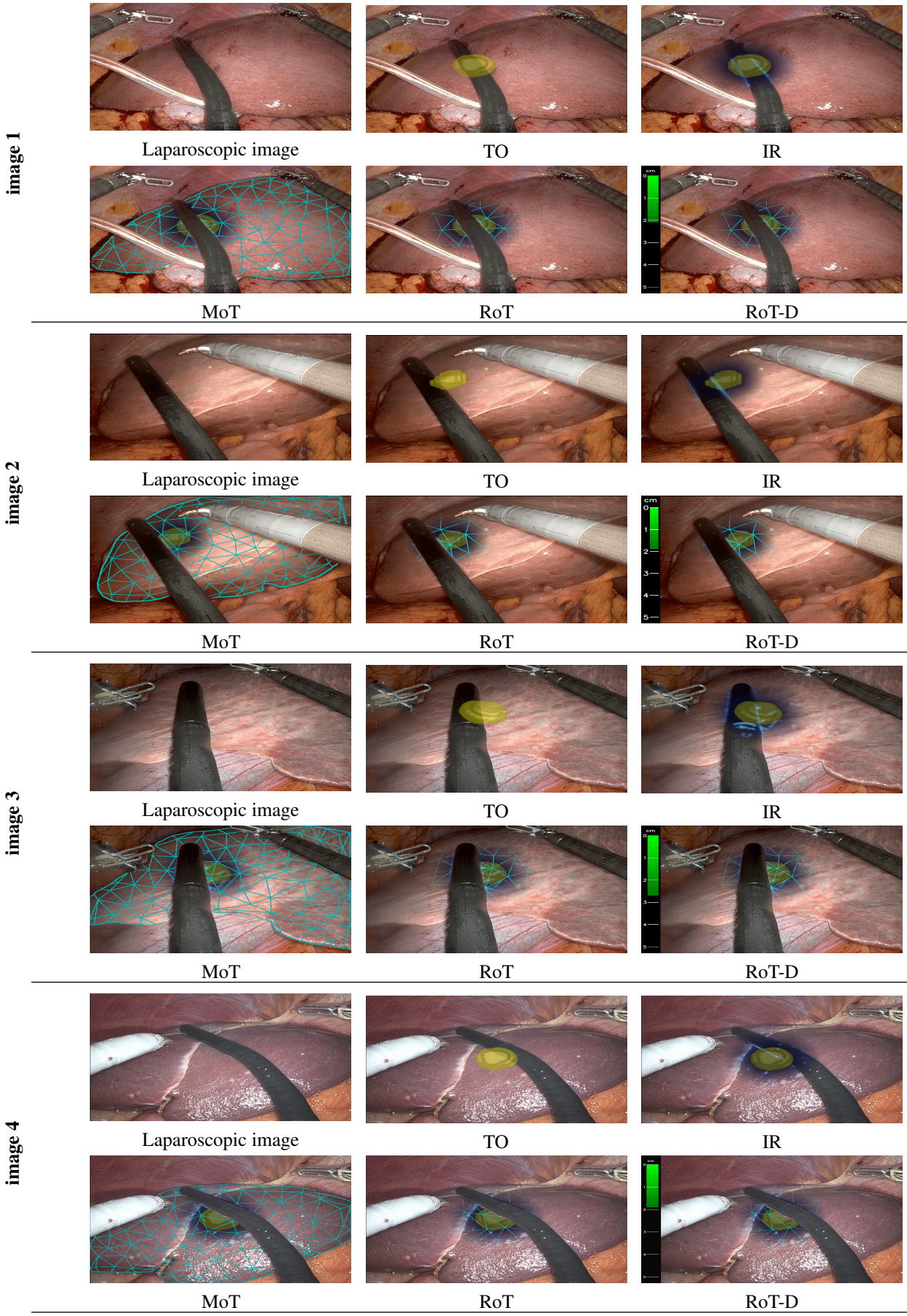

FIGURE 5 Visualizations for tumors occluded by a surgical instrument.

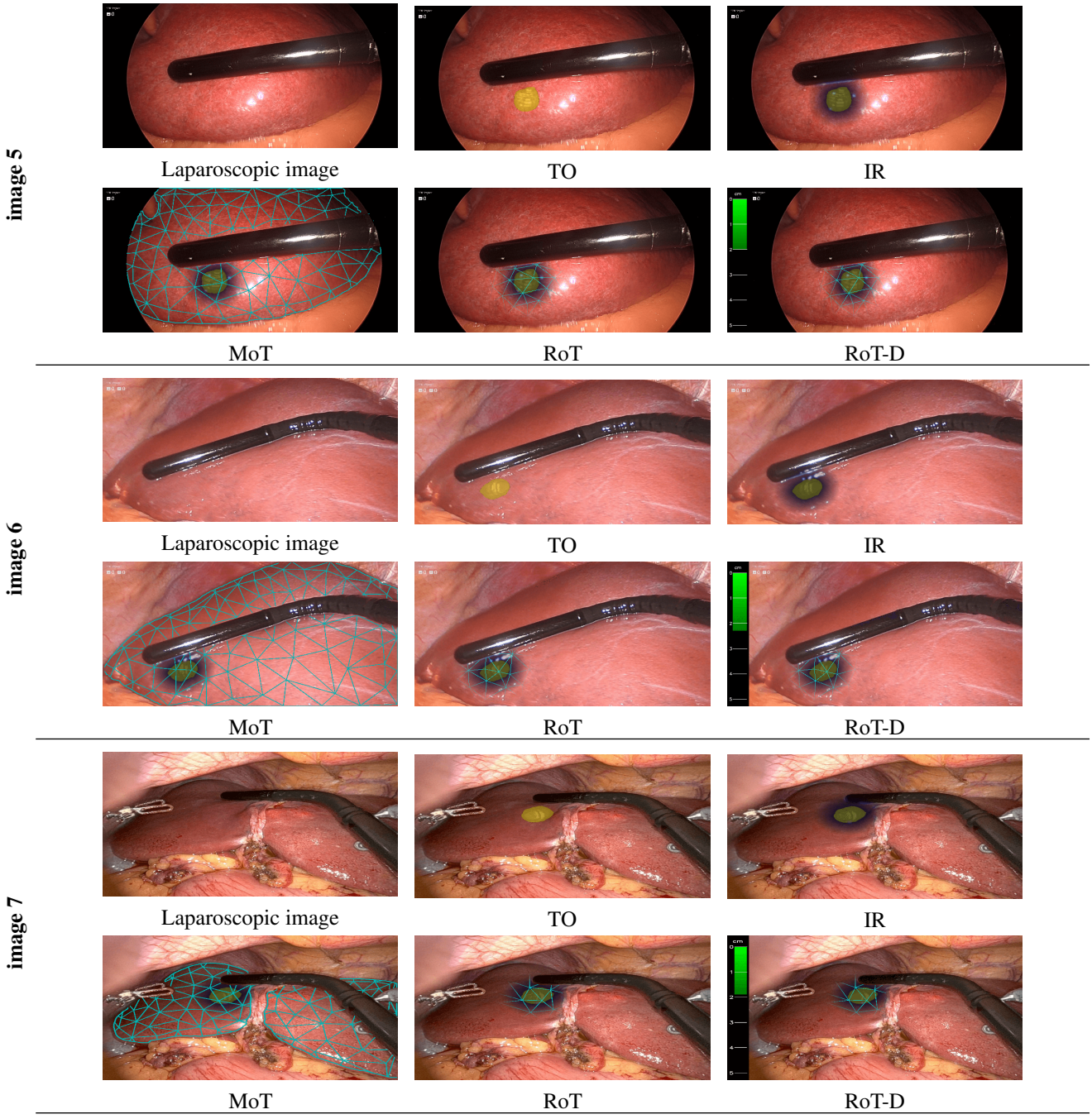

FIGURE 6 Visualizations for tumors not occluded by a surgical instrument.

Source of errors. There are four steps where errors might occur. *(i) Preperative 3D tumor model segmentation*. State-of-the-art segmentation methods achieve over 80% Dice score. However, this step can also be done manually by an expert before the surgery to further increase precision. *(ii) Intraoperative LUS image tumor segmentation*. State-of-the-art segmentation methods achieve 87% Dice score (*e.g.*,[15]). *(iii) Intraoperative LUS probe pose estimation*. State-of-the-art pose estimation methods achieve sub-millimeter accuracy (*e.g.*,[14]). *(iv) Rigid tumor registration between LUS and CT*. State-of-the-art registration methods achieve 3 *mm* TRE (*e.g.*,[3]). Overall, the state of the art methods for each part of the proposed pipeline reach reasonable accuracies, with regularly improving performance over the years.

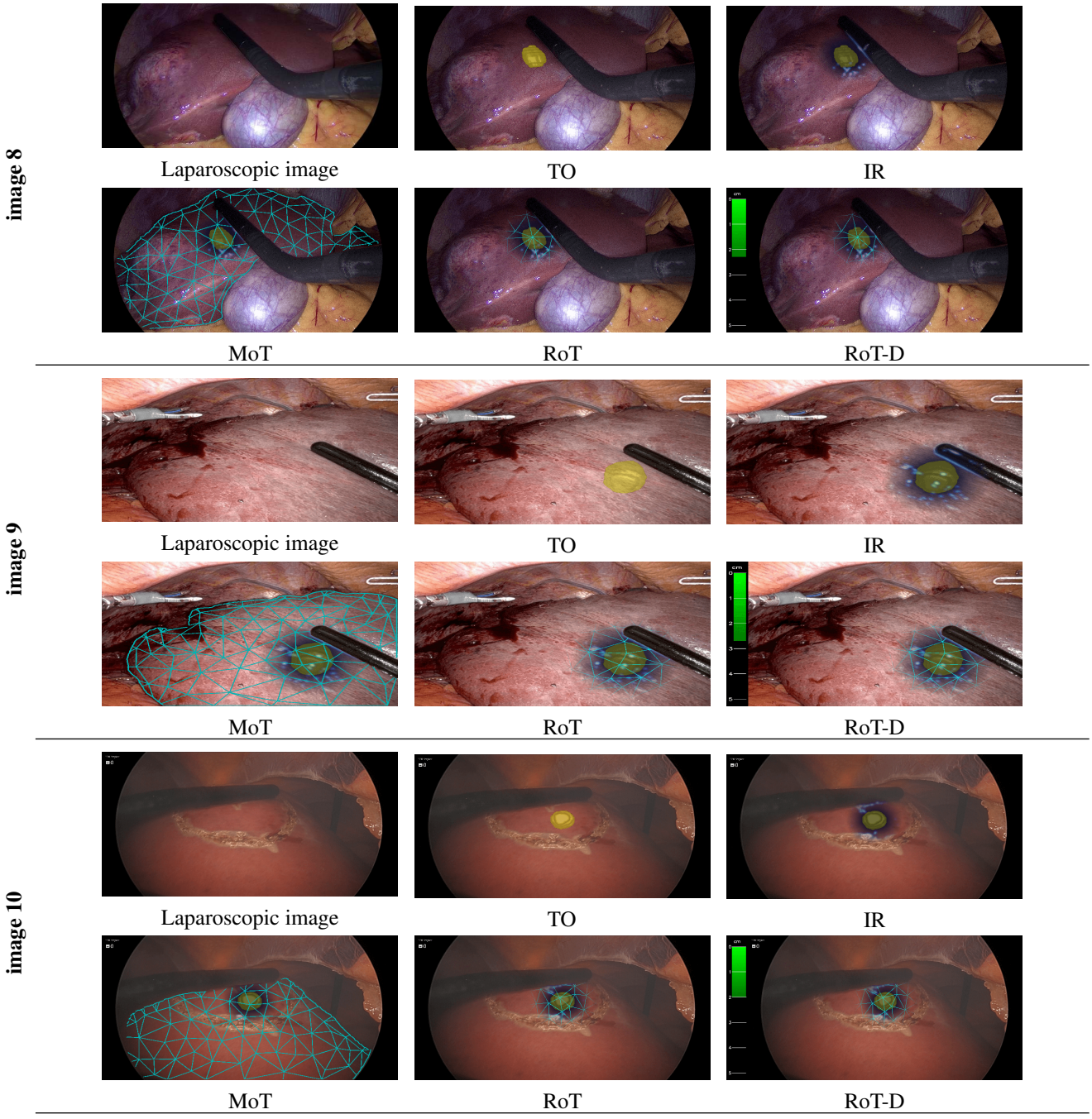

FIGURE 7 Visualizations for tumors with imperfect liver segmentation.

4 | USER STUDY ON VISUALIZATIONS AND RESULT

We conducted a user study to compare MoT, RoT, and RoT-D visulazations against the Transparent Overlay (TO) visualization [3,4,5,6,7,8,9,10,11] and the Inverse Realism (IR) visualization [12].

Visualization cases. We used 10 laparoscopic liver images. Each image was retrieved from a different liver resection surgery. This helps evaluate the visualization methods across 10 diverse cases. These cases are shown in figures 5, 6 and 7.

User study. We removed the methods' names. Instead, we used "Visualization 1" for TO, "Visualization 2" for IR, "Visualization 3" for MoT, "Visualization 4" for RoT, and "Visualization 5" for RoT-D. Participants read the following: "We propose 5 different hidden tumor visualizations for cases from 10 different surgeries. Please vote for the best visualization". Participants then voted.

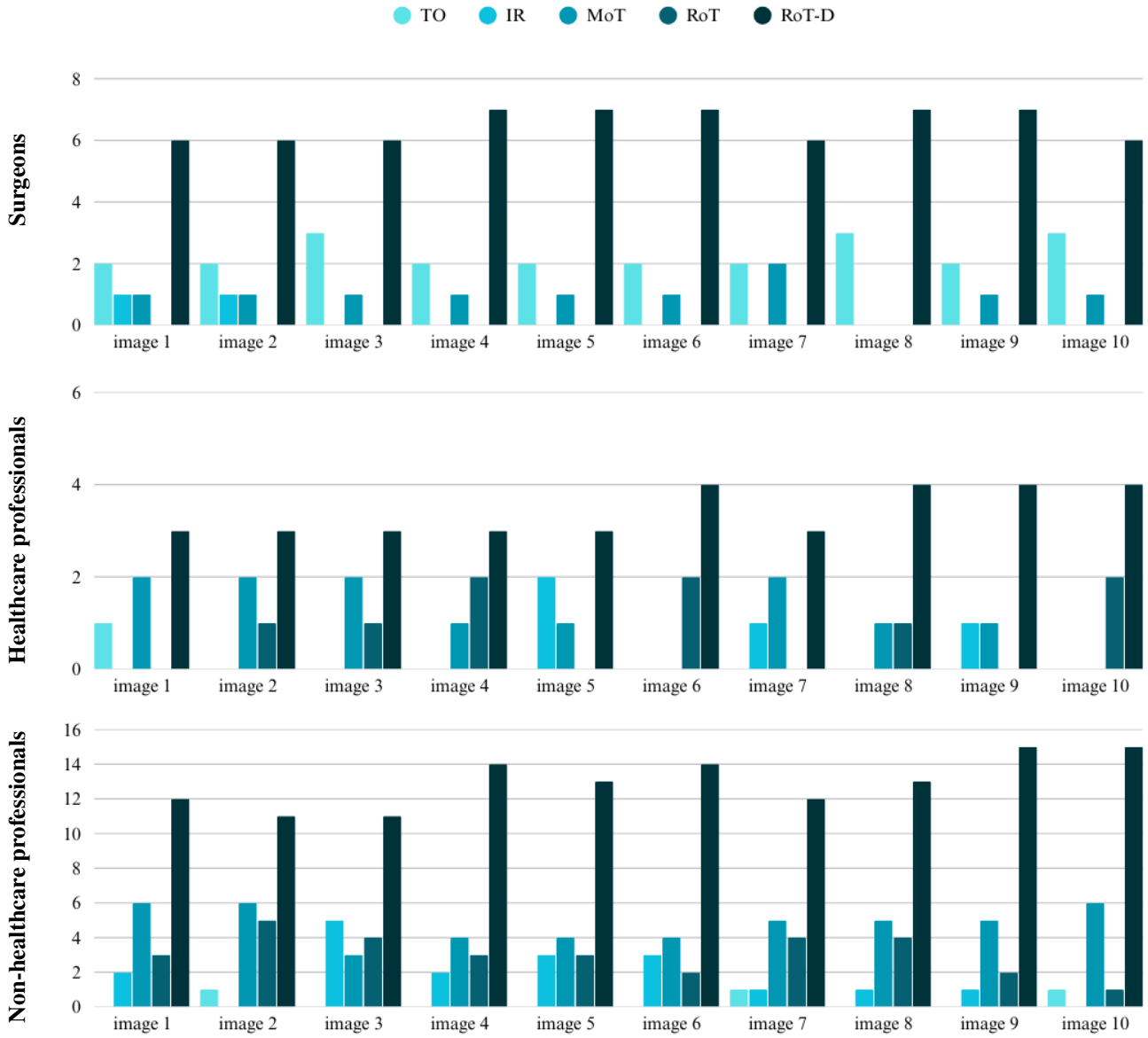

FIGURE 8 User study results.

Participants. 39 people participated in the study. Participants include surgeons, healthcare professionals, and non-healthcare professionals.

Surgeons. 10 participants were surgeons. 7 were laparoscopic liver surgeons. 2 were laparoscopic surgeons operating within the abdominal cavity. 1 was laparoscopic surgeon operating outside the abdominal cavity. 4 of them were senior surgeons with more than 4 years of experience.

Healthcare professionals. 6 participants were healthcare professionals.

Non-healthcare professionals. 23 participants were non-healthcare professionals. They are researchers in the field of computer vision applied to medical augmented reality.

Results on all cases. The user study results are shown in figure 8 for the surgeons, healthcare professionals and non-healthcare professionals. The results reveal that RoT-D outperforms the other visualizations in all cases. See figure 9 for an example of RoT-D. TO came as runner-up in surgeons' votes. This shows that surgeons also prefer less cluttered visualizations. MoT came as runner-up in healthcare and non-healthcare professionals' votes. This shows that the liver's visible surface mesh corrects the spatial depth perception of the tumor. Surgeons preferred "Visualization 5" (RoT-D) across all images, and among their remarks was that the depth indicator bar provides critical information.

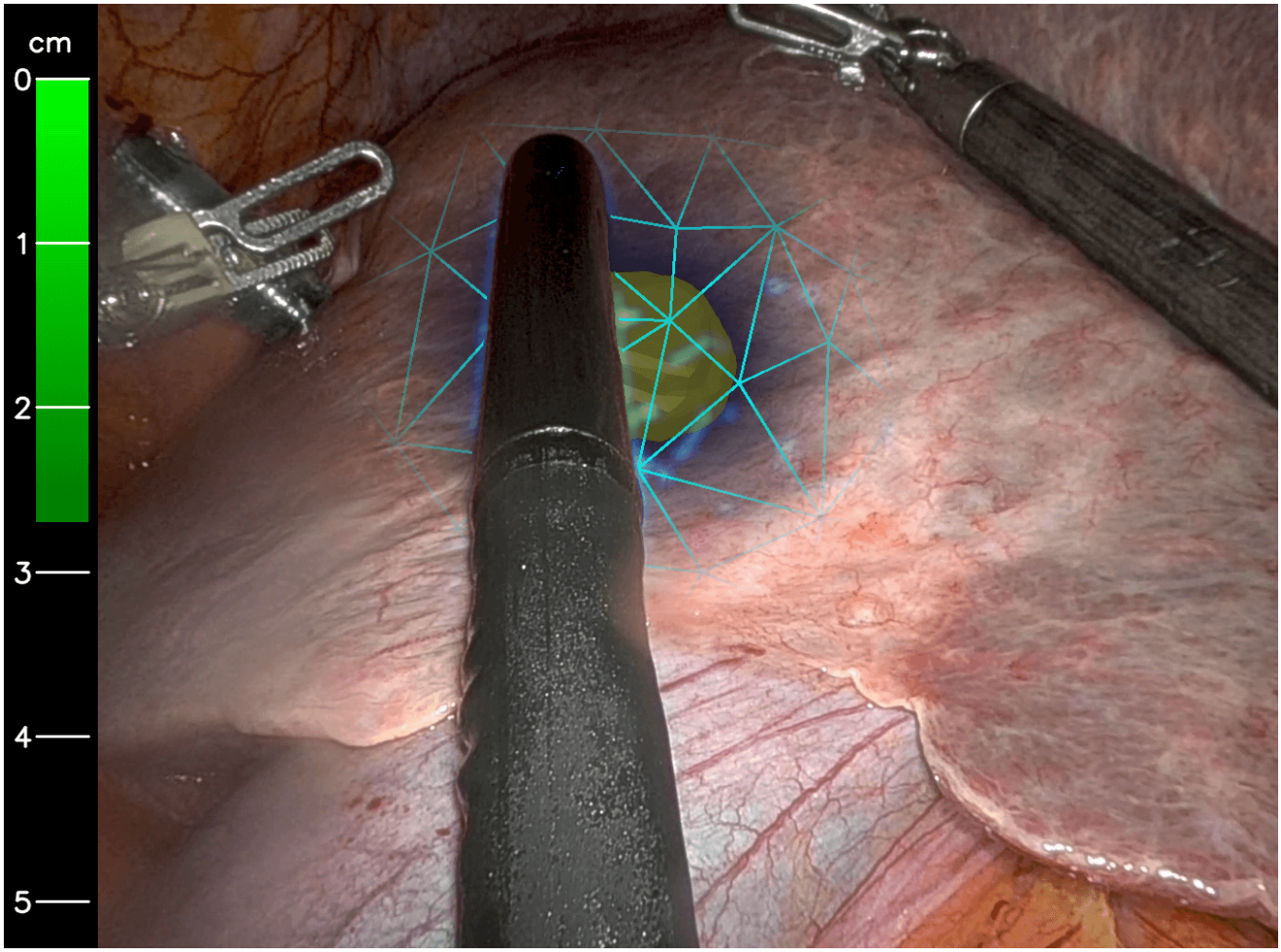

FIGURE 9 An example for the winner visualization RoT-D.

Results on cases where tumors were occluded by an instrument. The user study in figure 8 reveals that for cases shown in figure 5, RoT-D substantially outperforms the other methods.

Results on cases where tumors were not occluded by an instrument. The user study in figure 8 reveals that in the three cases shown in figure 6, RoT-D outperforms the other methods even when the tumor is not occluded by an instrument.

Results on cases where the liver's segmentation was imperfect. The user study in figure 8 reveals that in the three cases shown in figure 7, RoT-D outperforms the other methods even for images that are underexposed or cluttered by blood.

5 | USER STUDY ON DEPTH ESTIMATION AND RESULTS

We conducted a user study to evaluate depth estimations of the tumor using RoT visualization.

Depth estimation cases. We used 4 laparoscopic liver images from 4 different patients to generate RoT visualizations of the registered tumors. These four cases are shown in figure 10.

User study. We asked the participants to estimate the depth of the tumors in these four cases in centimeter units. The depth bars were not shown to the participants.

Participants. The same 10 surgeons participated to this user study.

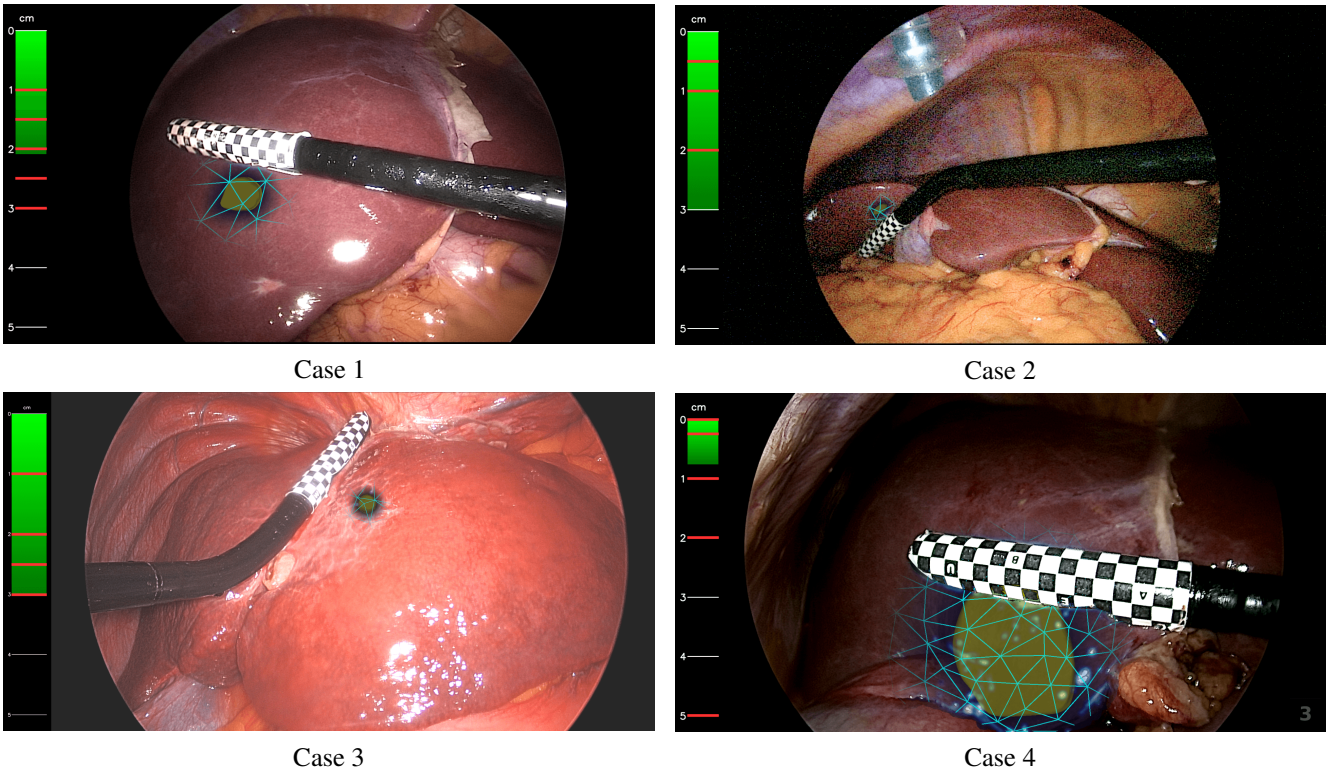

FIGURE 10 User study on tumor depth estimations. The depth bars are not shown to the users while they were making the estimates. Multiple depth estimates have the same value and their red lines are superimposed on the depth indicator bars.

Results. The estimated depths by the surgeons are shown as red horizontal lines on the depth bars of each visualization in figure 10 and listed in table 1. Table 1 reveals that *(i)* the surgeons' estimates are consistent, except for case 4 which has higher standard deviation and *(ii)* the average errors are large, except for case 1 which is about 5%. Therefore, we observe that tumor depth estimations from 2D laparoscopic images are unreliable.

TABLE 1 User study on tumor depth estimations using RoT visualization.

	GT depths (cm)	**10 surgeons' depth estimates** (cm)										**Mean** $\pm$ **Std** (cm)	**Relative errors**
Case 1	2.09	2	3	3	2.5	2	3	2	2	1	1.5	2.2 ± 0.64	5%
Case 2	3.02	1	1	1	1	2	1	1	2	0.5	0.5	1.1 ± 0.49	63%
Case 3	2.40	3	2	2	2	1	2	1	1	2	2.5	1.9 ± 0.63	20%
Case 4	0.76	2	2	0	1	1	1	6	5	0.2	0.2	1.8 ± 1.96	136%

6 | CONCLUSION

We have proposed a novel visualization method with three visualization variants named MoT, RoT and RoT-D, for hidden tumors in liver laparoscopy. As opposed to existing methods requiring deformable registration to account for the complete parenchyma, we only require registration of the tumor, which can be expressed rigidly owing to its higher stiffness, resulting in a simpler

problem with stabler outcomes. This makes the proposed visualization method more applicable. It can be seamlessly applied to multiple subsurface structures, including multiple tumors and the vascularisation; for simplicity, however, we have discussed and experimented with the single tumor case only. A user study has shown that the proposed RoT-D visualization significantly improves the hidden tumor's depth perception in various surgical scenes compared to state-of-the-art tumor visualizations.

Future work shall *(i)* study segmentation of the gall-bladder, falciform ligament, and blood pixels to improve the liver's outlines in the visualization, *(ii)* study tracking of the liver's mesh across successive images to prevent flickering in the visualizations, *(iii)* study real-time implementability, *(iv)* study extension to other organs, *(v)* conduct phantom and ex-vivo studies to quantitatively assess the accuracy, robustness, and clinical usability of the proposed visualization method, *(vi)* evaluate tumor depth estimations from the proposed visualizations (excluding ROT-D) against the known absolute depths, and *(vii)* study the visualization of the tumor's depth accuracy.

7 | ACKNOWLEDGEMENT

This work is funded by project ANR JCJC - IMMORTALLS.

REFERENCES

1. Singla R, Edgcumbe P, Pratt P, Nguan C, Rohling R. Intra-operative ultrasound-based augmented reality guidance for laparoscopic surgery. *Healthc. Technol. Lett.*. 2017;4(5):204–209.
2. Le Roy B, Ozgur E, Koo B, Buc E, Bartoli A. Augmented reality guidance in laparoscopic hepatectomy with deformable semi-automatic computed tomography alignment (with video). *J. Visc. Surg.*. 2019;156(3):261–262.
3. Ramalhinho J, Tregidgo HF, Gurusamy K, Hawkes DJ, Davidson B, Clarkson MJ. Registration of untracked 2D laparoscopic ultrasound to CT images of the liver using multi-labelled content-based image retrieval. *IEEE Transactions on Medical Imaging.* 2020;40(3):1042–1054.
4. Cipolato O, Fauconneau M, LeValley PJ, Nißler R, Suter B, Herrmann IK. An augmented reality visor for intraoperative visualization, guidance, and temperature monitoring using fluorescence. *J. Biophotonics.* 2025;18(2):e202400417.
5. Tortolero LB, Hajtovic SA, Gautreaux J, Lebowitz R, Placantonakis DG. Intraoperative augmented reality visualization in endoscopic transsphenoidal tumor resection using the Endoscopic Surgical Navigation Advanced Platform (EndoSNAP): A technical note and retrospective cohort study. *Cureus.* 2025;17(2):e79714.
6. Lecointre L, Verde J, Goffin L, et al. Robotically assisted augmented reality system for identification of targeted lymph nodes in laparoscopic gynecological surgery: a first step toward the identification of sentinel node : Augmented reality in gynecological surgery. *Surg. Endosc.*. 2022;36(12):9224–9233.
7. Solbiati M, Ierace T, Muglia R, et al. Thermal ablation of liver tumors guided by augmented reality: An initial clinical experience. *Cancers (Basel).* 2022;14(5):1312.
8. Evans M, Kang S, Bajaber A, Gordon K, Martin C. Augmented Reality for Surgical Navigation: A review of advanced needle guidance systems for percutaneous tumor ablation. *Radiol. Imaging Cancer.* 2025;7(1):e230154.
9. Van Gestel F, Frantz T, Buyck F, et al. Neuro-oncological augmented reality planning for intracranial tumor resection. *Front. Neurol..*;14:1104571.
10. Javaheri H, Ghamarnejad O, Bade R, Lukowicz P, Karolus J, Stavrou GA. Beyond the visible: preliminary evaluation of the first wearable augmented reality assistance system for pancreatic surgery. *Int. J. Comput. Assist. Radiol. Surg.*. 2025;20(1):117–129.
11. Louis RG, Steinberg GK, Duma C, et al. Early experience with virtual and synchronized augmented reality platform for preoperative planning and intraoperative navigation: A case series. *Oper. Neurosurg. (Hagerstown).* 2021;21(4):189–196.
12. Lerotic M, Chung AJ, Mylonas G, Yang GZ. Pq-space based non-photorealistic rendering for augmented reality. *Medical Image Computing and Computer-Assisted Intervention – MICCAI.* 2007:102–109.
13. Collins T, Pizarro D, Gasparini S, et al. Augmented reality guided laparoscopic surgery of the uterus. *IEEE Transactions on Medical Imaging.* 2020;40(1):371–380.
14. Kalantari MM, Ozgur E, Alkhatib M, et al. LARLUS: laparoscopic augmented reality from laparoscopic ultrasound. *Int. J. Comput. Assist. Radiol. Surg.*. 2024;19(7):1285–1290.
15. Natali T, Zhylka A, Olthof K, et al. Automatic hepatic tumor segmentation in intra-operative ultrasound: a supervised deep-learning approach. *J Med Imaging.* 2024;11(2).
16. Saha A, Pol v. dCB. Liver observation segmentation on contrast-enhanced MRI: SAM and MedSAM performance in patients with probable or definite hepatocellular carcinoma. *Can. Assoc. Radiol. J.*. 2024;75(4):771–779.
17. Chang C, Law H, Poon C, et al. Segment Anything Model (SAM) and medical SAM (MedSAM) for lumbar spine MRI. *Sensors (Basel).* 2025;25(12):3596.
18. Nazzal W, Thurnhofer-Hemsi K, López-Rubio E. Improving medical image segmentation using test-time augmentation with MedSAM. *Mathematics.* 2024;12(24):4003.
19. Li B, Liu B, Yao X, Yue J, Zhou F. Advancing Depth Anything Model for unsupervised monocular depth estimation in endoscopy. 2024.
20. Yang L, Kang B, Huang Z, Xu X, Feng J, Zhao H. Depth Anything: Unleashing the Power of Large-Scale Unlabeled Data. In: 2024:10371-10381.
21. Teatini A, Frutos P. dJ, Eigl B, et al. Influence of sampling accuracy on augmented reality for laparoscopic image-guided surgery. *Minim. Invasive Ther. Allied Technol.*. 2021;30(4):229–238.
22. Heiliger C, Heiliger T, Deodati A, et al. Phantom study on surgical performance in augmented reality laparoscopy. *Int. J. Comput. Assist. Radiol. Surg.*. 2023;18(8):1345–1354.
23. Wang H, Yang G, Zhang S, et al. Video-Instrument Synergistic Network for referring video instrument segmentation in robotic surgery. *IEEE Trans. Med. Imaging.* 2024;43(12):4457–4469.

24. Sheng Y, Bano S, Clarkson MJ, Islam M. Surgical-DeSAM: Decoupling SAM for Instrument Segmentation in Robotic Surgery. Preprint; 2024.
25. Labrunie M, Pizarro D, Tilmant C, Bartoli A. Automatic 3D/2D Deformable Registration in Minimally Invasive Liver Resection using a Mesh Recovery Network. *Medical Imaging with Deep Learning.* 2024;227:1104–1123.
26. Mhiri I, Pizarro D, Bartoli A. Neural patient-specific 3D-2D registration in laparoscopic liver resection. *Int. J. Comput. Assist. Radiol. Surg.*. 2025;20(1):57–64.
27. Awais M, Altaie M, O'Connor C, Castelo A, Tran Cao H, Brock K. Real-time vasculature segmentation during laparoscopic liver resection using attention-enriched U-Net model in intraoperative ultrasound videos. *SPIE Medical Imaging.* 2024.
28. Koo B, Özgür E, Le Roy B, Buc E, Bartoli A. Deformable registration of a preoperative 3D liver volume to a laparoscopy image using contour and shading cues. *Medical Image Computing and Computer Assisted Intervention – MICCAI.* 2017:326–334.
29. Adagolodjo Y, Trivisonne R, Haouchine N, Cotin S, Courtecuisse H. Silhouette-based pose estimation for deformable organs application to surgical augmented reality. *IEEE/RSJ International Conference on Intelligent Robots and Systems – IROS.* 2017:539–544.